

Quantum and classical localization in the lowest Landau level

Nancy Sandler,* Hamid R. Maei, and Jané Kondev

Department of Physics, Brandeis University, Waltham, Massachusetts 02454, USA

(Received 5 September 2003; published 20 November 2003)

Spatial correlations of occupation probabilities, if their decay is not too fast, can change the critical exponents for classical percolation. From numerical studies of electron dynamics in the lowest Landau level (LLL) we demonstrate the quantum analog of this effect. Similar to classical percolation, we find that the extended Harris criterion applies to localization in the LLL. These results suggest experiments that might probe new quantum critical points in the integer quantum Hall setting.

DOI: 10.1103/PhysRevB.68.205315

PACS number(s): 73.43.Nq, 64.60.Ak, 71.30.+h

I. INTRODUCTION

Quantum or classical dynamics can lead to localization of a particle moving in a random environment. The localized state in the quantum case is described by a wave function which spreads over a finite distance, the localization length. In the classical case particle trajectories are closed orbits limited in extent. The mechanism by which localization can occur in the two settings is very different as quantum interference, which plays a crucial role in quantum localization, has no classical counterpart. In this paper we report on the intriguing relation between classical and quantum localization in the setting of the integer quantum Hall (IQH) effect, when a power-law correlated disorder potential is present.

The problem of localization in the IQH setting has been studied since the effect was first discovered. Localization is believed to be responsible for the plateaus in the Hall resistance which are observed as a function of the applied magnetic field.¹ Transitions between adjacent plateaus have been identified with a zero-temperature quantum critical point² which is characterized by the divergence of the localization length as the magnetic field is tuned to its critical value. Support for this picture is provided by observations of critical scaling in experiments of Wei *et al.*³ and Koch *et al.*,⁴ which found a localization length exponent $\nu_q \approx 2.3$.

Theoretical studies of localization in the IQH system usually take the semiclassical picture⁵ as their starting point. Here the electron's motion is split into the fast cyclotron rotation and the slow $\mathbf{E} \times \mathbf{B}$ drift of the guiding center along lines of constant electrostatic potential. The potential $V(\mathbf{r})$, caused by impurities, is assumed to be random. Quantum mechanics enters at the saddle points of the potential where the electron can tunnel from one equipotential orbit to another, while the perpendicular magnetic field results in a random Aharonov-Bohm phase between two tunnelling events. A lattice model which describes the network of saddle points was introduced by Chalker and Coddington,⁶ and it leads to a value of the localization exponent consistent with experiments.

The classical limit of the network model corresponds to percolation.⁷ The classical trajectories are equipotential lines of $V(\mathbf{r})$, which can be mapped to the hulls of percolation clusters.⁸ However, little is known about quantum localization when the classical limit is described by correlated percolation. Namely, as shown by Weinrib,⁹ power-law correla-

tions of the random potential can change the percolation critical point leading to a different fractal geometry of its equipotential lines. This happens when the exponent α , which characterizes the spatial decay of the potential correlations [see Eq. (5)] satisfies $\alpha < 2/\nu_c$; $\nu_c = 4/3$ is the correlation length exponent for percolation.¹⁰ Here we investigate the effect that changing the fractal geometry of classical trajectories, has on quantum localization in the IQH system. We find new localization critical points when $\alpha < 2/\nu_q$, i.e., the quantum analog of correlated percolation. (This problem was previously studied by Cain *et al.* using real space renormalization group techniques, but no definite proof of the effect was found.¹¹)

II. QUANTUM DYNAMICS IN THE LOWEST LANDAU LEVEL

The Hamiltonian for two-dimensional spinless electrons confined to the x - y plane, and under the combined effects of a magnetic field $\mathbf{B} = B\hat{z}$ and a random potential $V(\mathbf{r})$, is $H = 1/2m(\mathbf{p} - e\mathbf{A})^2 + \sum_{\mathbf{k}} V_{-\mathbf{k}}\rho_{\mathbf{k}}$. Here \mathbf{A} is the vector potential, $\rho_{\mathbf{k}} = e^{i\mathbf{k}\cdot\mathbf{r}}$ is the one-particle density operator and $V_{\mathbf{k}}$ is the Fourier transform of the disorder potential. At high magnetic fields (or low temperatures), the quantum dynamics of the electron are governed by the projection of the Hamiltonian onto the lowest Landau level (LLL)

$$\hat{H} = \sum_{\mathbf{k}} V_{-\mathbf{k}} \hat{\rho}_{\mathbf{k}}, \quad (1)$$

where $\hat{\rho}$ is the projected density operator. We focus our attention on the localization properties of the eigenfunctions of \hat{H} . Previous numerical studies¹² indicate that the localization length increases towards the center of the LLL band, with a localization length exponent $\nu_q \approx 7/3$. In these studies the random potential was assumed to be short range correlated. Here we take up the question of how power-law correlated potentials might affect the value of ν_q .

Recently, Sinova *et al.*¹³ have shown that the localization length exponent can be computed from the disorder averaged density-density correlation function projected onto the LLL. It was further shown by Gurarie and Zee¹⁴ that the classical limit of the time evolution of this correlation function describes electron drift along the equipotentials of $V(\mathbf{r})$, as expected. These results lead to a simple scaling argument for

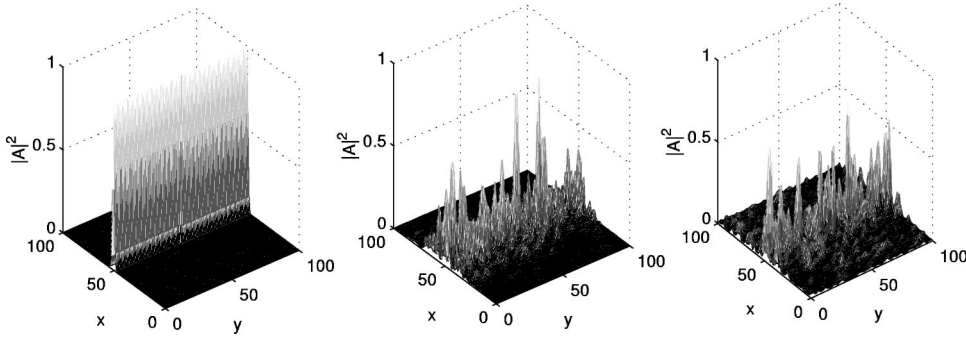


FIG. 1. Evolution of a wave packet composed of all eigenstates and initially localized at $x=0.5$. $A(x,y)$ is the wave packet amplitude.

the subdiffusive spreading of wave packets in the lowest Landau level.¹⁵ Namely, start by assuming that the disorder potential completely breaks the degeneracy of the LLL, leaving only one extended state at energy $E_c=0$. Let us examine the time evolution of a wavepacket $|\psi_E(t)\rangle$ constructed from localized eigenstates of Eq. (1) that are taken from an interval of width Δ centered around E . The dispersion of this wavepacket, $\langle \Delta x^2(t) \rangle_E \equiv \langle \psi_E(t) | x^2 | \psi_E(t) \rangle$, is expected to be diffusive for short times [$t \ll \xi^2(E)/D$, D = diffusion constant], attaining a constant value set by the localization length $\xi(E)$ at long times. This can be summarized by a scaling form

$$\overline{\langle \Delta x^2(t) \rangle_E} = Dt f\left(\frac{Dt}{\xi^2(E)}\right), \quad (2)$$

where the bar denotes disorder averaging and f is a scaling function, with properties $f(x) \rightarrow \text{const}$ for $x \ll 1$, and $f(x) \rightarrow \text{const}/x$ for $x \gg 1$. Now, if we construct a wave function in the LLL as a superposition of the wave packets $|\psi_E(t)\rangle$ its dispersion can be written as

$$\overline{\langle \Delta x^2(t) \rangle} \approx \sum_{E \rightarrow -\infty}^{E=0} \overline{\langle \Delta x^2(t) \rangle_E}, \quad (3)$$

where the contributions of the nondiagonal terms can be neglected since only the state at $E=0$ is extended. Replacing $\overline{\langle \Delta x^2(t) \rangle_E}$ by Eq. (2), making use of $\xi(E) \sim E^{-\nu_q}$, and the nonsingular nature of the density of states for $E \rightarrow 0$, we obtain

$$\overline{\langle \Delta x^2(t) \rangle} \sim (Dt)^{1-1/2\nu_q}. \quad (4)$$

Therefore, the spread of the wave function at late times is subdiffusive due to the presence of the extended eigenfunction at the band center, and the anomalous diffusion exponent $\theta = 1 - 1/2\nu_q$. This forms the basis of the numerical method we use below to compute ν_q .

III. POWER-LAW CORRELATED DISORDER POTENTIAL

To study quantum dynamics and localization in the LLL in the presence of power-law correlated disorder potentials, we make use of the Hamiltonian in Eq. (1) with $V(\mathbf{k})$ a random Gaussian variable with zero mean and variance given by $|\mathbf{k}|^{\alpha-2}$. After Fourier transforming this leads to a potential which is power-law correlated in real space

$$\langle V(\mathbf{r})V(\mathbf{0}) \rangle \propto \frac{1}{|\mathbf{r}|^\alpha}. \quad (5)$$

The projected Hamiltonian matrix is written in the basis of states given by the Landau eigenstates on the torus, which in the Landau gauge can be written as

$$\begin{aligned} \psi_l(x,y) = & \sum_{m=-\infty}^{\infty} \exp\left(2\pi i \frac{y}{L}(Nm+l)\right) \\ & \times \exp\left(-\pi \frac{N}{L^2} \left[x - \frac{L}{N}(l+Nm)\right]^2\right). \end{aligned} \quad (6)$$

Here l goes from 0 to $N-1$, labeling the N states on the torus, N is the number of flux quanta through the torus, and L is the system size. These wave functions are defined on $[0,L) \times [0,L)$, they are centered at $x=Ll/N$ and have appreciable amplitude in a narrow strip of width given by the magnetic length $l_c = \sqrt{L^2/2\pi N}$. [Below we set $L=1$, rendering (x,y) dimensionless.]

The electron density operator $\hat{\rho}(k_1, k_2) = \exp[2\pi i(k_1 x + k_2 y)]$ projected onto the LLL is a matrix of the form

$$\hat{\rho}(k_1, k_2) = \exp\left(-\frac{k_1^2 + k_2^2}{2N}\pi\right) L(k_1, k_2), \quad (7)$$

where k_1, k_2 are integers in the units chosen, $[(k_1, k_2) \neq (0,0)]$, and the matrix elements of $L(k_1, k_2)$ are given by

$$[L(k_1, k_2)]_{l_1, l_2} = e^{2\pi i[k_1 k_2/2 + k_1(l_1-1)]/N} \delta_{l_1, l_2 - k_2} \Big|_{\text{mod } N}. \quad (8)$$

(The formalism used to project the density operator $\rho_{\mathbf{k}}$ onto the LLL was developed in Ref. 16.)

For a given realization of $V(\mathbf{r})$, the eigenvectors and eigenvalues of \hat{H} are obtained by exact diagonalization.¹⁷ A wave packet localized along x is made using all the eigenstates. As it evolves it spreads, and its width in the x direction is computed as a function of time. For one realization of the short-range correlated random potential, Fig. 1 shows a set of snapshots for the evolution of a wave packet initially localized at $x=0.5$. To obtain $\overline{\langle \Delta x^2(t) \rangle}$ the width of the wave packet is averaged over all initial positions and over 1000 different disorder realizations; Eq. (4) is then used for computing ν_q .

First, we checked this numerical procedure for a short-range correlated disorder potential, where the Fourier com-

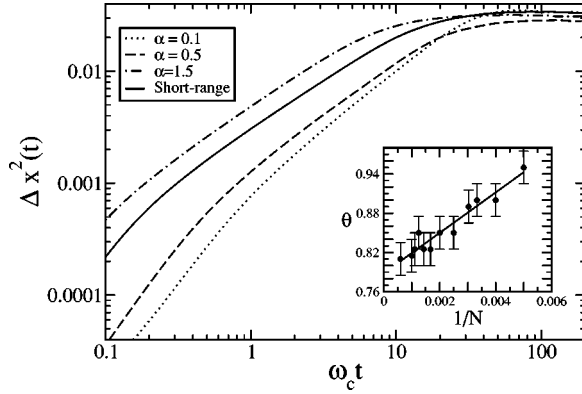


FIG. 2. Disorder averaged spread of the wave packet, for $N = 1000$ basis states in the LLL, as a function of time, and for different disorder potentials. Anomalous diffusion is evident at intermediate times. Inset: The exponent θ for different values of N in the case of a short-range correlated disorder potential.

ponents of $V(\mathbf{r})$ (in units of $\hbar\omega_c$) are independent and uniformly distributed on the interval $[-0.5, 0.5]$. The value of $\theta = 1 - 1/2\nu_q$ is given by the slope of $\langle \Delta x^2(t) \rangle$ when plotted on a log-log graph. To take into account finite size effects we repeat the computation of θ for $200 \leq N \leq 1500$ and plot it as a function of $1/N$; see inset of Fig. 2. By linear extrapolation we find $\nu_q = 2.33(9)$ in the $N \rightarrow \infty$ limit, consistent with previous results. We then repeat the computation for long-range correlated disorder potentials for different values of the parameter α . Results are shown in Fig. 2.

For each $\langle \Delta x^2(t) \rangle$ curve in Fig. 2, three regions can be identified. Due to the finite system size, at long enough times the spread of the wave packet reaches a constant value which corresponds roughly to 70% of the system size. The critical region corresponds to intermediate times, while the short time behavior is described by the slope $\theta \approx 2$. Ballistic motion ($\theta = 2$) follows from a perturbative calculation of $\langle \Delta x^2(t) \rangle$ at short times.¹⁸ Comparison among different $\langle \Delta x^2(t) \rangle$ curves shows that the value of the slope in the critical region begins to increase for $\alpha < \alpha^* \approx 0.75 - 0.80$.

IV. EXTENDED HARRIS CRITERION

The effect of short-range correlated disorder on a critical point is summarized by the Harris criterion.¹⁹ The criterion states that critical exponents for the disordered and the clean system remain equal as long as the value of the correlation length exponent ν satisfies $d\nu - 2 \geq 0$, where d is the dimensionality of the system under consideration. It is derived by demanding that the fluctuations of the random potential within a volume set by the correlation length do not grow faster than its average value, as the transition is approached. An extension of the criterion was proposed by Weinrib and Halperin²⁰ to include power-law correlated disorder potentials, similar to that in Eq. (5). When applied to two-dimensional percolation this ‘‘extended Harris criterion’’ reads⁹

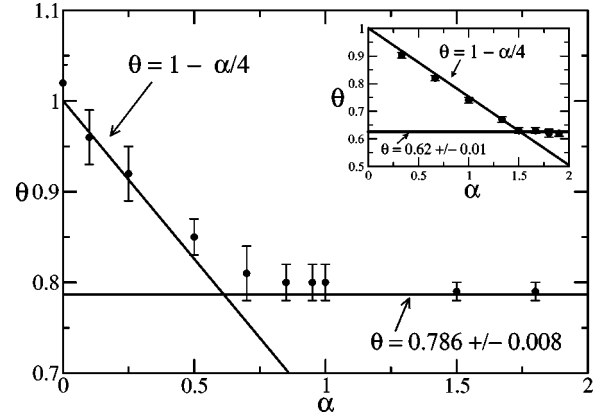


FIG. 3. The anomalous diffusion exponent $\theta = 1 - 1/2\nu_q$ characterizes the spread of a wave packet in the LLL. The power α describes the long-range nature of the correlations of the random potential. Full lines are theoretical curves obtained from the extended Harris criterion. The inset shows analogous results for the case of classical electron motion (Ref. 18).

$$\alpha > \alpha^* \Rightarrow \nu_c = \frac{2}{\alpha^*}, \quad \alpha < \alpha^* \Rightarrow \nu_c = \frac{2}{\alpha}, \quad (9)$$

where $\alpha^* = 3/2$. However, there is to our knowledge no evidence of the validity of the extended Harris criterion for quantum critical points. Since the localization transition in the LLL is believed to be the quantum counterpart of the classical percolation transition, it provides an ideal testing ground for the applicability of the criterion in the quantum realm.

With this in mind we calculate the value of the anomalous diffusion exponent $\theta = 1 - 1/2\nu_q$ by computing the value of θ in the critical region for different values for the degeneracy of the LLL, ranging from $N = 330$ to $N = 1000$, and then extrapolating to $N \rightarrow \infty$. Results from this computation, as well as the theoretical prediction based on the extended Harris criterion are shown in Fig. 3. In the quantum case the criterion reads as written in Eq. (9) except now $\alpha^* = 2/\nu_q = 0.786(8)$. In the inset of Fig. 3 we also show results of numerical analysis of classical electron motion in the same long-range correlated random potential, and compare to the prediction from the extended Harris criterion.¹⁸ The classical results were reported previously in Ref. 21. Our data confirm the validity of the extended Harris criterion for both quantum and classical electron dynamics in the LLL.

The main result of this paper is contained in Fig. 3. From the striking resemblance between classical and quantum behavior, we conclude that disorder correlations affect in a qualitatively similar way quantum and classical percolation. Indeed, the quantum version of the extended Harris criterion can be argued in close analogy with its classical counterpart. In this case we should consider the fluctuations of the random potential in a volume set by the localization length $\xi(E) \sim E^{-\nu_q}$, and compare them to E . The calculation that follows¹⁸ exactly parallels that done by Weinrib and Halperin,²⁰ and Eq. (9) follows with ν_q replacing ν_c .

An interesting consequence of the applicability of the extended Harris criterion to the IQHT, is the conclusion that the

simple relation between the classical and quantum localization length exponent, $\nu_q = \nu_c + 1$,²² cannot be valid in general. According to the quantum version of Eq. (9), for a long-range correlated disorder with $0.8 \leq \alpha \leq 1.5$ the quantum localization exponent will be the same as in the case of short-range correlated disorder while the classical one will vary continuously with α .

V. CONCLUSION

We conclude by speculating about a possible experimental test of our findings. The random potential present in samples that exhibit the IQH effect is thought to be short-range correlated, due to the nature of the spatial distribution of impurities within the heterojunction.¹ However, the effect of a random magnetic field in the presence of a much stronger constant magnetic field is equivalent to that of a random potential.²³ This opens up the possibility of engineering the properties of the disordered environment seen by the electrons, by applying a random magnetic field. This was, for example, demonstrated in Ref. 24 using a magnetic material with a rough contact surface placed in close proximity to the

electron layer. The height fluctuations of the material surface, and hence the correlations in the random field, can, in principle, be controlled by adjusting the growth conditions under which the material is made. Magnetic decoration techniques or magnetic force microscopy can be used to determine spatial correlations of the field and thus extract the value of α . At $T \approx 25$ mK, the saturated width of the Hall conductance step is $\Delta B \approx 0.5$ T for AlGaAs/GaAs structures. The temperature and ΔB place limits on the size of the random field fluctuations, which should roughly be in the interval $10^{-3} \text{ T} \leq \delta B \leq 10^{-1} \text{ T}$. Whether or not magnetic materials with these properties can be prepared, and placed in close proximity to the two-dimensional electron gas so as to effect its dynamics, remains to be seen.

ACKNOWLEDGMENTS

It is a pleasure to acknowledge useful conversations with B. Halperin, J. Sinova, V. Gurarie, S. Boldyrev, J. Moore, and S. Simon. J.K. was supported by the NSF under Grant No. DMR-9984471, and by the Research Corporation.

*Current address: Department of Physics and Astronomy, Ohio University, Ohio, OH 45701.

¹*The Quantum Hall Effect*, edited by R.E. Prange and S.M. Girvin (Springer-Verlag, New York, 1990).

²H. Levine, S.B. Libby, and A.M.M. Pruisken, Phys. Rev. Lett. **51**, 1915 (1983).

³H.P. Wei, D.C. Tsui, M.A. Paalanen, and A.M.M. Pruisken, Phys. Rev. Lett. **61**, 1294 (1988).

⁴S. Koch, R.J. Haug, K. von Klitzing, and K. Ploog, Phys. Rev. Lett. **67**, 883 (1993).

⁵S.A. Trugman, Phys. Rev. B **27**, 7539 (1983).

⁶J.T. Chalker and P.D. Coddington, J. Phys. C **21**, 2665 (1988).

⁷D.-H. Lee, Z. Wang, and S.A. Kivelson, Phys. Rev. Lett. **70**, 4130 (1993).

⁸M. Isichenko, Rev. Mod. Phys. **64**, 961 (1992).

⁹A. Weinrib, Phys. Rev. B **29**, 387 (1984).

¹⁰M.P.M. den Nijs, J. Phys. A **12**, 1857 (1979).

¹¹P. Cain, R.A. Römer, M. Schreiber, and M.E. Raikh, Phys. Rev. B **64**, 235326 (2001).

¹²B. Huckestein, Rev. Mod. Phys. **67**, 357 (1995), and references

therein.

¹³J. Sinova, V. Meden, and S.M. Girvin, Phys. Rev. B **62**, 2008 (2000).

¹⁴V. Gurarie and A. Zee, Int. J. Mod. Phys. B **15**, 1225 (2001).

¹⁵S. Boldyrev and V. Gurarie, J. Phys.: Condens. Matter **15**, L125 (2003).

¹⁶S. Girvin and T. Jach, Phys. Rev. B **29**, 5617 (1984).

¹⁷W.H. Press, B.P. Flannery, S.A. Teukolsky, and W.T. Vetterling, *Numerical Recipes in C* (Cambridge University Press, Cambridge, 1988).

¹⁸N. Sandler, H. Maei, and J. Kondev (unpublished).

¹⁹A.B. Harris, J. Phys. C **7**, 1671 (1974).

²⁰A. Weinrib and B.I. Halperin, Phys. Rev. B **27**, 413 (1983).

²¹S. Prakash, A. Havlin, M. Schwartz, and H.E. Stanley, Phys. Rev. A **46**, R1724 (1992).

²²G.V. Mil'nikov and I.M. Sokolov, JETP Lett. **48**, 536 (1989).

²³B. Huckestein, Phys. Rev. B **53**, 3650 (1995).

²⁴L. Zielinski, K. Chaltikian, K. Birnbaum, C.M. Marcus, K. Campman, and A.C. Gossard, Europhys. Lett. **42**, 73 (1998).